International Journal of Modern Physics D

Neutrino-pair interactions in astrophysical systems

María Paula Colombi, Osvaldo Civitarese and Ana V. Penacchioni
Dept. of Physics, University of La Plata, c.c. 67, (1900) La Plata, Argentina
E-mail: osvaldo.civitarese@fisica.unlp.edu.ar

We study the effects produced by interactions among neutrinos upon extra-galactic neutrino-fluxes. We have assumed a separable type of pair interactions and performed a transformation to a quasi-particle mean field followed by a Tamm-Damcoff diagonalization. In doing so, we have adopted techniques originated in the quantum many-body problem, and adapted them to this specific case. The solutions of the associated eigenvalue problem provide us with energies and amplitudes which are then used to construct the neutrino response functions at finite density and temperature. The formalism is applied to the description of neutrinos produced in a SN environment.

Keywords: Extragalactic, neutrinos, collectivity, supernovae

26.60.+c, 26.50.+x, 13.15.+g, 13.15.+g, 03.75.Nt

1. Introduction

Neutrinos play an important role in the collapse and explosion of massive stars. They carry information from the heart of the explosion, which we couldn't acquire through photons or other particles [1]. Besides, due to their weakly interacting nature, they can provide us with insights into the dynamics and thermodynamics at the center of a supernova (SN) [2]. Neutrinos are generated in a variety of astrophysical scenarios [3]. Core-collapse SN are among the most powerful sources of neutrinos in our Universe. During a SN explosion, 99% of the emitted energy ($\sim 10^{49} - 10^{53}$ erg) is released by neutrinos (ν) and antineutrinos ($\bar{\nu}$) that are formed from neutrons and protons through β-decay. These astrophysical messengers pass straight through the collapsing star before the explosion takes place. Their detection provides an early warning prior to the arrival of the electromagnetic signal [4]. Other extragalactic progenitors include gamma-ray bursts (GRB), which may originate from binary systems [5] such as two neutron stars (NS) or a NS and a black hole (BH), some active galactic nuclei (AGN), especially blazars and, last but not least, the Big Bang [6].

Extragalactic neutrinos (and antineutrinos) are created through different mechanisms according to the characteristics of their progenitors. There are no charged current interactions of ν with the medium. Instead, there is a variety of neutral current interactions, e.g.:

- $e^- - e^+$ pair annihilation:

$$e^- + e^+ \rightarrow \nu_e + \bar{\nu_e}.$$

  This mechanism typically occurs in the first stages of a collapsar GRB explosion. Due to vacuum polarization, $e^- - e^+$ pairs are created. A fraction of the pairs annihilate to photons, while another fraction gives rise to $\nu - \bar{\nu}$ pairs.
- β-decay:

$$n \rightarrow p + e^- + \bar{\nu_e}.$$

  This usually occurs in neutron rich systems, such as NS.
- Inverse β-decay:

$$p \rightarrow n + e^+ + \nu_e.$$

- p-p interaction: this consists in the interaction of a relativistic proton from a GRB jet with a cold proton from the outermost shells of the expanding star. Charged pions are produced as a result of the interaction, which later decay giving neutrinos (antineutrinos)

$$\pi^+ \rightarrow \mu^+ + \nu_\mu,$$

$$\pi^- \rightarrow \mu^+ \bar{\nu_\mu}.$$

- p-γ interaction: a relativistic proton from the GRB jet interacts with a less energetic photon, i.e. a synchrotron photon. This again produces charged mesons that decay into ν and $\bar{\nu}$ through the channels just mentioned above.

There are also other neutrino production mechanisms such as plasmon decay, photoannihilation, bremsstrahlung, neutronization, etc [7, 8].

Although the exact value of the neutrino mass is still unknown, it is clear that neutrino mass is many orders of magnitude smaller than the mass of their leptonic partners. This makes it possible for neutrino oscillations to take place. When a beam of neutrinos travels through space, the proportion of each flavor (e, μ and τ) changes, and so the amount of neutrinos arriving at the detectors on Earth in each flavor state is different from the one at the source.

Concerning neutrino detection, there are several technologies, some currently running and others planned for the future. Water Cherenkov detectors employ water (liquid or solid) as the detection material. When neutrinos pass through a water tank they produce Cherenkov light that is collected by photomultiplier tubes. Super-Kamiokande (SK) [9] is a typical detector of this kind. Recently, Gd was introduced in the detector in order to enhance neutron-tagging efficiency and try to achieve the first observation of SN relic neutrinos (SRN) or diffuse SN neutrino background. [10]. Hyper-Kamiokande (HK) [11] is to be the next generation of large-scale water Cherenkov detectors. It is planned to be an order of magnitude bigger than SK. Ice Cube [12], located in the South Pole, is another kind of Cherenkov detector that

works in the sub-TeV to EeV energy range. It is continuously monitoring the full sky to detect astrophysical neutrinos, and it regularly alerts other experiments in near real-time about interesting neutrino observations in order to enable electromagnetic follow-up observations.

Most current detectors are sensitive primarily to $\bar{\nu}_e$. The reason is that the main detector materials for large underground detectors are rich in free protons, which have a rather large (and well known) cross section for interaction with $\bar{\nu}_e$ via inverse β-decay, with a threshold of $E_{\nu_{thr}} = 1.8$ MeV [13].

SN neutrino spectra have a rich structure, since different energy groups emerge from different depths in the proto-NS atmosphere. However, on a rough level of approximation, the overall spectrum follows a thermal distribution. The mean energy of the distribution ranges from a few to tens of MeV [14].

So far, neutrinos have been treated as a gas, but since the neutrino density is of the order of nuclear matter density ($\rho_0 = 2.8 \times 10^{14}$ g/cm^3) [15], interactions among them may take place [16, 17] and collective phenomena may arise. In this work we are considering neutrino-pair interactions to study possible observational consequences.

The work of Birol et al [18] explored some features of the neutrino system by applying quantum many-body techniques. Working with an effective two-flavor mixing scenario under the single-angle approximation, they presented a solution based on the Richardson-Gaudin diagonalization scheme [19]. It was a crucial step towards the understanding of the role of ν-ν interactions beyond the independent-particle approach.

Concerning the many body aspects of the present calculations, in addition to [18], the work of Ref. [20] treats ν-ν interactions in the context of the RPA, applying the Bethe Ansatz. The obtained eigenstates and eigenvalues were then used to build the neutrino linear response. The interaction used in [20] is of the schematic form. This formulation has the advantage of separability, and it allows to distinguish effects due to mean-field (BCS-type) and residual two-body correlations.

Concerning the astrophysical aspects of the system which we are addressing here, namely, the study of the effects due to ν-ν interactions in the interior of a supernova upon the spectral function of the neutrino, we shall refer to the work of Y. Pehlivan et al [21]. There, the effects of the neutrino interactions both in the superfluid (BCS) and condensed (BEC) regimes were considered. The authors of Ref. [21] gave a clear picture about the density dependence of the effects attributed to neutrino interactions, since they took into account the density variations between the inner and outer shells of the supernova. In Ref. [21], the suitability of the many-body concepts applied to the neutrino interactions was based in the analogy with other many-body systems, like the atomic nucleus and hadrons in QCD.

A major difficulty found when applying many-body techniques to the neutrino interactions is related to dimensionality. The Bethe Ansatz method used in Ref. [20] show numerical instabilities for large dimensions. A way out to circunvent this problem has been explored in Ref. [22]. It consists in implementing a variational

approach and expressing the Bethe Ansatz equations in a differential form, yielding a set of algebraic equations. The procedure used in Ref. [22] illustrates clearly the differences between the mean-field and exact solutions for extended systems of spin-$\frac{1}{2}$ particles. It represents a nice step forward towards a deeper understanding of the role of ν-ν interactions in astrophysical scenarios.

The work of C. Volpe [23] reviews some of the methods which are currently employed to treat ν-ν interactions in astrophysical systems. Particular emphasis is placed on the discussion of the mean-field method, its extensions, and the use of Boltzmann equations. As stated in Ref. [23], since the equations of motion are non-linear, the inclusion of corrections due to pairing and spin correlations requires some care. The author presents as well a path integral approach to the neutrino many-body problem.

To summarise the main points of Refs. [20–23] in connection with our work, we shall emphasize the role of the many-body degrees of freedom in dealing with the neutrino system, and the plausibility of the application of common techniques from other branches of Physics to assess the competition between mean-field and collective effects.

Following the ideas of the references cited above, we have developed a description of collective effects resulting from neutrino-pair interactions. As a first step, we perform a transformation to a quasi-particle basis. The particle degrees of freedom in the superfluid basis are then the neutrino-equivalent to the standard quasi-particles, e.g. quasi-neutrinos. Pairs of neutrinos in the superfluid regime are treated in the framework of the Tamm-Dancoff approximation (TDA) [24]. With the corresponding response function evaluated at finite density and temperature we investigate the changes in the flux of neutrinos due to ν-ν interactions.

The paper is organised as follows: in Section 2 we introduce the formalism, which is then applied to a system of SN-neutrinos. The results of the calculations are presented and discussed in Section 3. Finally, in Section 4, we draw our conclusions.

2. Formalism

2.1. *Non-interacting neutrinos: energy distribution*

The SN neutrinosphere may be considered as a blackbody emitter in which neutrinos are in equilibrium at temperature T. If neutrinos are taken as free particles, their number distribution is given by the Fermi-Dirac statistics:

$$f(\varepsilon, T) = \frac{1}{e^{(\varepsilon-\mu)/T} + 1}, \tag{1}$$

where ε is the neutrino energy in the relativistic ($\varepsilon = \sqrt{p^2c^2 + m^2c^4}$) or ultrarelativistic ($\varepsilon = pc$) regime, μ is the chemical potential and the temperature T is given in units of energy ($k_B = 1$).

Taking continuous momentum eigenvalues and an ultrarelativistic dispersion

relation, their density and total energy per unit volume are given by

$$\rho = \frac{g_s}{2\pi^2 (\hbar c)^3} \int_0^\infty d\varepsilon\, \varepsilon^2 f(\varepsilon, T) \tag{2}$$

and

$$E = \frac{g_s}{2\pi^2 (\hbar c)^3} \int_0^\infty d\varepsilon\, \varepsilon^3 f(\varepsilon, T)\,, \tag{3}$$

respectively, where $g_s = 2$ is the spin degeneracy factor. From the above equations we write the neutrino number distribution per unit energy

$$dN(\varepsilon, T) = \frac{1}{\rho}\frac{d\rho}{d\varepsilon} \tag{4}$$

and the number of neutrinos per unit energy

$$d\Phi(\varepsilon, T) = \frac{1}{E}\frac{dE}{d\varepsilon}\,, \tag{5}$$

both at a fixed T.

2.2. *Neutrino-pair interactions*

When neutrino densities reach those of nuclear matter, ν-ν interactions become relevant. To model this interactions in the simplest way, we add to the free Hamiltonian a number constraint (λN) and a contact interaction of the monopole pairing type:

$$H = H_{\text{free}} - \lambda N + V_{\text{pair}} = \sum_k (\varepsilon_k - \lambda) a_k^\dagger a_k - G \sum_{k,l>0} a_k^\dagger a_{\bar{k}}^\dagger a_{\bar{l}} a_l. \tag{6}$$

Here the indices k and l stand for the quantum numbers needed to specify a neutrino state, the operators $a_k^\dagger$ (a_k) create (annihilate) a neutrino in the state k, while $a_{\bar{k}}^\dagger$ ($a_{\bar{k}}$) create (annihilate) a neutrino in the time-reversed state $\bar{k}$. G is the state-independent strength of the interaction ($G > 0$).

The Hamiltonian (6) can be diagonalized by applying the Bogoliubov transformations to the quasi-particle basis:

$$\begin{aligned} \alpha_k^\dagger &= U_k a_k^\dagger - V_k a_{\bar{k}} \\ \alpha_{\bar{k}} &= U_k a_{\bar{k}} + V_k a_k^\dagger \\ \alpha_k &= U_k a_k - V_k a_{\bar{k}}^\dagger \\ \alpha_{\bar{k}}^\dagger &= U_k a_{\bar{k}}^\dagger + V_k a_k, \end{aligned} \tag{7}$$

where $\alpha_k^\dagger$ (α_k) create (annihilate) a quasi-particle state, U_k and V_k are occupation factors to be determined variationally, and since we are dealing with fermions, $U_k^2 + V_k^2 = 1$.

The Hamiltonian (6) is transformed to the quasi-particle basis (7), and normal-ordered with respect to the quasi-particle vacuum $|\text{BCS}\rangle$ ($\alpha|\text{BCS}\rangle = 0$), yielding

$$
\begin{aligned}
H_{00} &= -\frac{\Delta^2}{2G} + \sum_k \left(\varepsilon_k - \lambda\right) V_k^2 \\
H_{11} &= \sum_k \left[2\Delta U_k V_k + \left(\varepsilon_k - \lambda\right)\left(U_k^2 - V_k^2\right)\right] \alpha_k^\dagger \alpha_k \\
H_{20+02} &= \frac{1}{2}\sum_k \left[-\Delta\left(U_k^2 - V_k^2\right) + 2\left(\varepsilon_k - \lambda\right) U_k V_k\right]\left(\alpha_{\bar{k}}\alpha_k + \alpha_k^\dagger \alpha_{\bar{k}}^\dagger\right) \\
H_{22} &= -\frac{G}{2}\sum_{kl}\left(U_k^2 U_l^2 + V_k^2 V_l^2\right)\left(\alpha_k^\dagger \alpha_{\bar{k}}^\dagger \alpha_{\bar{l}}\alpha_l + \alpha_l^\dagger \alpha_{\bar{l}}^\dagger \alpha_{\bar{k}}\alpha_k\right) \\
H_{40+04} &= \frac{G}{4}\sum_{kl}\left(U_k^2 V_l^2 + U_l^2 V_k^2\right)\left(\alpha_k^\dagger \alpha_{\bar{k}}^\dagger \alpha_l^\dagger \alpha_{\bar{l}}^\dagger + \alpha_{\bar{k}}\alpha_l \alpha_{\bar{k}}\alpha_l\right),
\end{aligned} \tag{8}
$$

and terms which are proportional to the product of three creation and one annihilation operators, or viceversa. Such terms are irrelevant for the purpose of the present discussion. In the above equations, The energy gap Δ is given by

$$\Delta = G\sum_k U_k V_k. \tag{9}$$

To determine the quantities U_k, V_k and Δ, we follow the BCS method [25] and impose the conditions:

$$H_{11} = \sum_k E_k \alpha_k^\dagger \alpha_k \tag{10}$$

$$H_{20+02} = 0 \tag{11}$$

to diagonalize our Hamiltonian, at variance with the work by Birol et al. [18] in which the Richardson diagonalization was used instead. The BCS method leads to the expressions:

$$U_k^2 = \frac{1}{2}\left(1 + \frac{\varepsilon_k - \lambda}{E_k}\right) \tag{12a}$$

$$V_k^2 = \frac{1}{2}\left(1 - \frac{\varepsilon_k - \lambda}{E_k}\right), \tag{12b}$$

with the quasi-particle energy

$$E_k = \sqrt{(\varepsilon_k - \lambda)^2 + \Delta^2}. \tag{13}$$

The one-quasi-particle Hamiltonian is then written:

$$H_{\rm qp} = \sum_k E_k \alpha_k^\dagger \alpha_k. \tag{14}$$

The BCS formalism can also be used to describe neutrino-pair interactions at finite temperature. Following the rules of statistical mechanics we introduce the

thermal averages by taking traces with the statistical operator $e^{-H_{qp}/T}$, where H_{qp} is the one given in (14). Therefore, the quasi-particle occupation numbers $f_k(T) = \langle \alpha_k^\dagger \alpha_k \rangle$ are defined by:

$$\langle \alpha_k^\dagger \alpha_k \rangle = \frac{\mathrm{Tr}(\mathrm{e}^{-\mathrm{H_{qp}/T}} \alpha_\mathrm{k}^\dagger \alpha_\mathrm{k})}{\mathrm{Tr}(\mathrm{e}^{-\mathrm{H_{qp}/T}})}, \tag{15}$$

from where we get

$$f_k(T) = \frac{1}{e^{E_k/T} + 1}. \tag{16}$$

Proceeding analogously and taking traces with the transformed Hamiltonian (8), one gets the temperature-dependent version of the BCS quantities U_k, V_k, E_k and Δ [26]. The expression for the temperature-dependent gap is:

$$\Delta(T) = G \sum_k U_k V_k (1 - 2 f_k(T)). \tag{17}$$

Because of the temperature dependence of the gap Δ, the superfluid regime is restricted to the temperature range $0 \leq T \leq T_c$, where T_c is the critical temperature. For temperatures larger than T_c, the normal regime ($\Delta = 0$) is recovered. For $T < T_c$, and taking the limit in the continuum, the quasi-particle energy density per unit volume is written:

$$d\Phi_{qp} = \frac{g_s}{2\pi^2 (\hbar c)^3} \frac{E^3}{(e^{E/T} + 1)}, \tag{18}$$

where $E = \sqrt{(\varepsilon - \lambda)^2 + \Delta^2(T)}$.

2.3. *Collective excitations of neutrino pairs*

The next step in the treatment of neutrino-pair interactions consists of the diagonalization of the remaining terms of the Hamiltonian (8), namely $H_{22} + H_{40+04}$. We shall start with the Tamm-Dancoff approximation (TDA) applied to the Hamiltonian

$$H' = H_{qp} + H_{22}. \tag{19}$$

In order to do so, we introduce linear combinations of the quasi-neutrino pairs

$$\Gamma_n^\dagger = \sum_k X_k^{(n)} \alpha_k^\dagger \alpha_{\bar{k}}^\dagger. \tag{20}$$

The one-phonon operator $\Gamma_n^\dagger$ acts upon the quasi-particle vacuum creating a state $|n\rangle$ of energy ω_n

$$\Gamma_n^\dagger |\mathrm{BCS}\rangle = \omega_\mathrm{n} |\mathrm{n}\rangle$$

The amplitudes $X_k^{(n)}$ and the energies ω_n are determined by solving the TDA equation of motion [27]

$$[H', \Gamma_n^\dagger] = \omega_n \Gamma_n^\dagger. \tag{21}$$

The vacuum state in the TDA approach coincides with the BCS vacuum, the energies ω_n are the solutions of the dispersion relation

$$X_k^{(n)} = \frac{A_k^{(n)}}{2E_k - \omega_n}, \tag{22}$$

where

$$A_k^{(n)} = G \sum_{k'} \frac{F_{kk'}}{2E_{k'} - \omega_n} A_{k'}^{(n)} \tag{23}$$

and

$$F_{kk'} = U_k^2 U_{k'}^2 + V_k^2 V_{k'}^2. \tag{24}$$

The energies are then solution to

$$\mathrm{Det}(\mathbb{1} - \mathrm{F}(\omega_\mathrm{n})) = 0, \tag{25}$$

where $F(\omega_n)$ is the matrix whose elements are

$$[F(\omega_n)]_{kk'} = G \frac{F_{kk'}}{2E_{k'} - \omega_n}. \tag{26}$$

The extension of the formalism to finite temperatures is straightforward and it amounts to the replacements [26, 27]

$$F_{kk'} \to F_{kk'}(1 - 2f_{k'}(T)), \tag{27}$$

due to the fact that

$$[\alpha_{\bar{k}}\alpha_k, \alpha_{k'}^\dagger \alpha_{\bar{k}'}^\dagger] = \delta_{kk'}(1 - 2f_k(T)). \tag{28}$$

The inclusion of the term H_{40+04} would imply to adopt the Random-Phase Approximation (RPA) method, for which there will be a new vacuum $|\mathrm{RPA}\rangle$ different from the $|\mathrm{TDA}\rangle$ one and, consequently, the one-phonon operator takes the form

$$\Gamma_n^\dagger = \sum_k X_k^{(n)} \alpha_k^\dagger \alpha_{\bar{k}}^\dagger - Y_k^{(n)} \alpha_{\bar{k}} \alpha_k, \tag{29}$$

being

$$Y_k^{(n)} = \frac{B_k^{(n)}}{2E_k + \omega_n}. \tag{30}$$

The quantities $A_k^{(n)}$ and $B_k^{(n)}$ are solutions of the new system of equations

$$\begin{bmatrix} A^{(n)} \\ B^{(n)} \end{bmatrix} = \begin{bmatrix} F(\omega_n) & S(\omega_n) \\ R(\omega_n) & Z(\omega_n) \end{bmatrix} \begin{bmatrix} A^{(n)} \\ B^{(n)} \end{bmatrix} \tag{31}$$

where the matrices S, R and Z have the following elements:

$$\begin{aligned}
[F(\omega_n)]_{kk'} &= G\frac{F_{kk'}}{2E_{k'}-\omega_n},\\
[S(\omega_n)]_{kk'} &= -G\frac{L_{kk'}}{2E_{k'}+\omega_n},\\
[R(\omega_n)]_{kk'} &= -G\frac{L_{kk'}}{2E_{k'}-\omega_n},\\
[Z(\omega_n)]_{kk'} &= G\frac{F_{kk'}}{2E_{k'}+\omega_n}
\end{aligned} \tag{32}$$

and

$$L_{kk'} = U_k^2V_{k'}^2 + V_k^2U_{k'}^2. \tag{33}$$

The extension of the formalism to finite temperatures requires, as before, $F_{kk'} \to F_{kk'}(1-2f(T))$ and $L_{kk'} \to L_{kk'}(1-2f(T))$. The energies ω_n are now the solutions of the equation

$$\mathrm{Det}\begin{bmatrix} \mathbb{1}-F(\omega_n) & -S(\omega_n) \\ -R(\omega_n) & \mathbb{1}-Z(\omega_n)\end{bmatrix} = 0. \tag{34}$$

The amplitudes $X_k^{(n)}$ and $Y_k^{(n)}$, for each state with energy ω_n, are normalized to

$$\sum_k [(X_k^{(n)})^2 - (Y_k^{(n)})^2](1-2f_k(T)) = 1. \tag{35}$$

The TDA expressions are straightforwardly recovered by setting $Y_k^{(n)} = 0$, and the $T = 0$ case by writing $f_k(T=0) = 0$, for all values of k. The energy distribution both for the TDA and the RPA states obeys Bose statistics with occupation factors

$$b_n(T) = \frac{1}{e^{\omega_n/T}-1}. \tag{36}$$

Therefore, it follows that the discrete energy distribution will be given by

$$\sum_n \omega_n b_n(T). \tag{37}$$

In the limit of the continuum [28], for the spectrum ω_n, the energy distribution $\Phi(\omega)$ is proportional to

$$\Phi(\omega) \approx \frac{\omega^3}{e^{\omega/T}-1}. \tag{38}$$

3. Results

In this section we shall present and discuss the results of our calculations, which have been performed by adopting the following set of parameters shown in Table 3:

Symbol	Physical meaning	Value
ρ	Density of neutrinos	10^{30} neutrino/cm^3
r	Radius of the neutrinosphere	10^5 cm
T	Temperature	0-2 MeV
G	Strength of the ν-ν interaction	3.42×10^{-34} MeV

3.1. *Non-interacting neutrinos*

With the parameters given in Table 3 we have calculated the number distribution and the energy distribution for neutrinos with energies $E_k = \sqrt{p_k^2 c^2 + m^2 c^4}$. Since we have assumed $pc >> mc^2$, the Fermi energy at $T = 0$ is given by the expression

$$\varepsilon_F(T = 0, \rho) = (3\pi^2 \rho)^{1/3} \hbar c, \tag{39}$$

which gives a value of the order of 0.67 MeV for the value of ρ given in Table 3.

Applying the Fermi-Dirac statistics, Eq. 4 and Eq. 5, we have obtained the results shown in Figures 1-3. The curves shown in Figure 1 and Figure 2, for different temperatures, exhibit a displacement in the energy of the maxima, as the temperature increases. The broadening of the spectrum (Figure 2) extends to large neutrino energies. For typical SN temperatures ($T = 2$ MeV), the energy distribution reaches the maximum at $\varepsilon \approx 6 - 7$ MeV. Figure 3 shows the mean value of the energy per neutrino, as a function of the temperature. The curve follows a dependence of the type $E/N \propto T^2$.

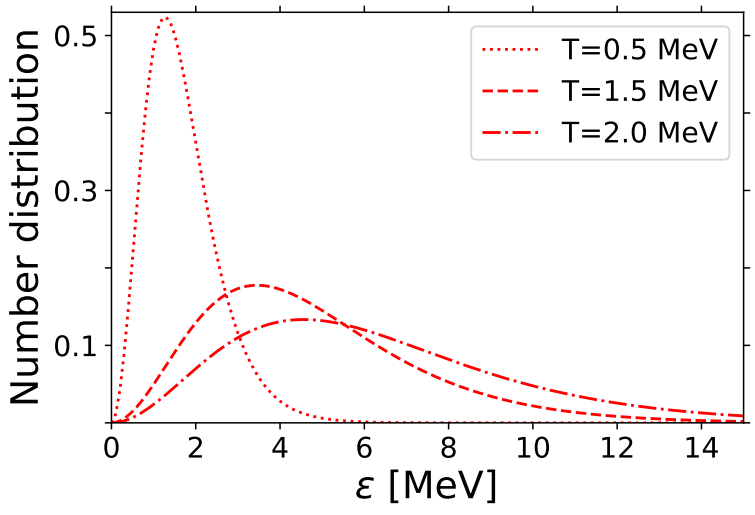

Fig. 1. Number distribution of free neutrinos (Eq. 4) as a function of the neutrino energy, for three different temperatures: $T = 0.5$ MeV (dotted line), $T = 1.5$ MeV (dashed line) and $T = 2$ MeV (dash-dotted line).

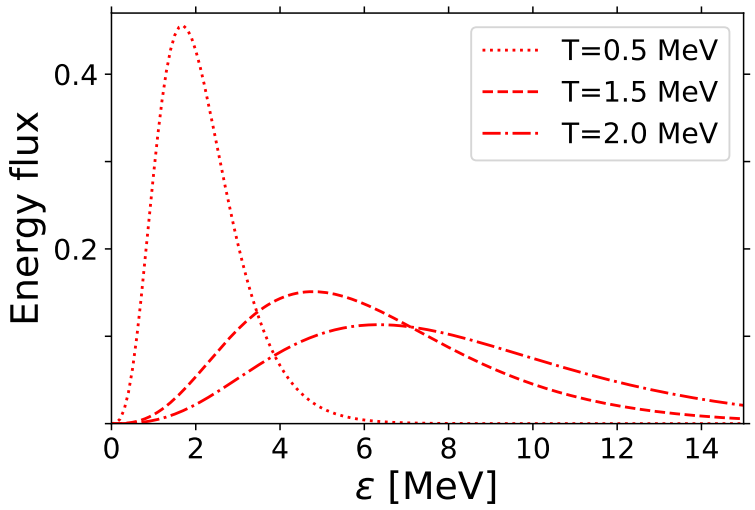

Fig. 2. Energy-flux of free neutrinos (Eq. 5) as a function of the neutrino energy, for three different temperatures: $T = 0.5$ MeV (dotted line), $T = 1.5$ MeV (dashed line) and $T = 2$ MeV (dash-dotted line).

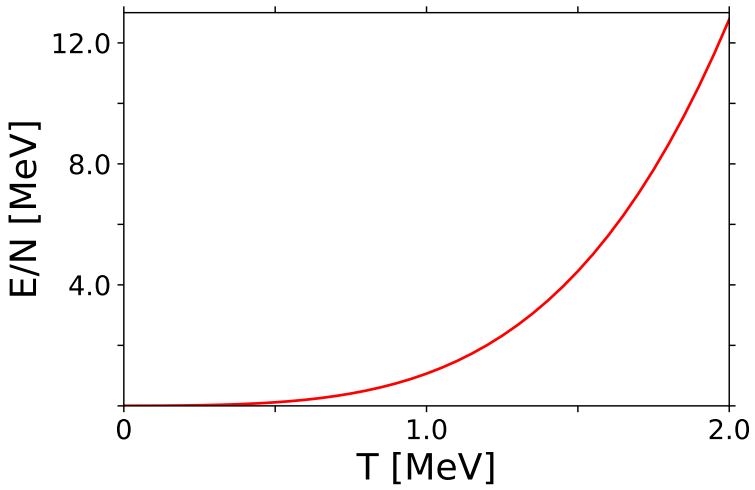

Fig. 3. Mean value of the energy per particle (Equation 3), for free neutrinos as a function of the temperature.

3.2. *Neutrinos in the quasi-particle representation*

As mentioned in the introduction, the treatment of neutrinos at high densities by means of pair interactions has been advanced in [18]. Here, we are adopting the same notion by working with the BCS approach.

Using the formalism presented in Section 2.2, requiring that ρ be high enough so that neutrinos in the neutrinosphere may interact pairwise, the solutions of the BCS equations lead to the properties of the neutrinos as quasi-particles.

Figure 4 shows the behaviour of the gap as a function of the temperature, as given by $\Delta(T)$ in Eq. 17. The gap collapses at the critical temperature $T = T_c$ which, for the present case, is of the order of 1.75 MeV.

In Figure 5 we show the quasi-particle excitation energy given by the expectation value of the Hamiltonian (10) for different values of the temperature. It has the typical 'S' shape reminiscent of a first-order phase-transition. For temperatures below T_c, the energy grows slowly. When the temperature increases, and the energy gap decreases (see Figure 4), lower energy states become activated and eventually the system seemingly undergoes a first order phase transition at $T = T_c$ and reaches the normal phase for higher values of T (see Figure 3). Although the concept of phase transitions does not apply to systems with finite number of degrees of freedom, for the present case the values of the density and cutoff in momentum space are sufficiently large to justify its use. The critical temperature determines the transition between the superfluid ($T < T_c$) and the normal ($T > T_c$) regime, as mentioned before.

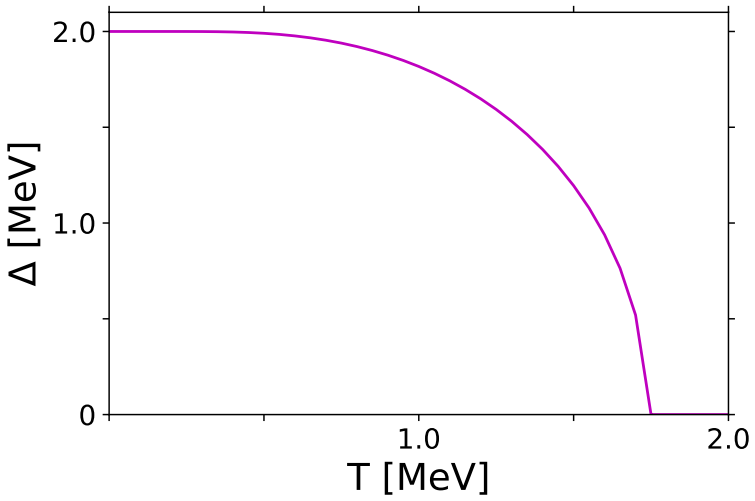

Fig. 4. Dependence of the energy gap (Eq. 17) with temperature.

Figure 6 shows the quasi-particle energy flux as a function of the energy, for three different values of the temperature. At low temperatures ($T = 0.5$ MeV), the spectrum has a threshold at 2 MeV. This feature persists at higher temperatures ($T = 1.5$ MeV) below T_c although the threshold reduces to about 1 MeV. For temperatures higher than T_c ($T = 2$ MeV), the threshold disappears and the spectrum

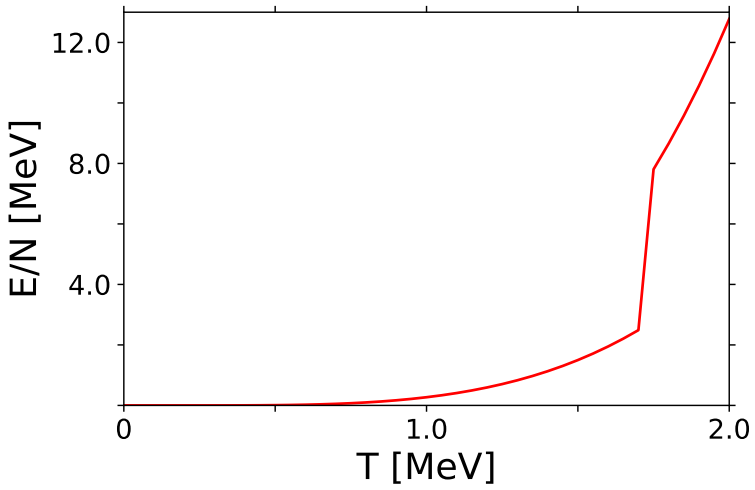

Fig. 5. BCS excitation energy as a function of the temperature, i.e, the mean value of the Hamiltonian (10), E/N, calculated as a function of the temperature T.

regains the structure found in the normal phase (see Figure 2).

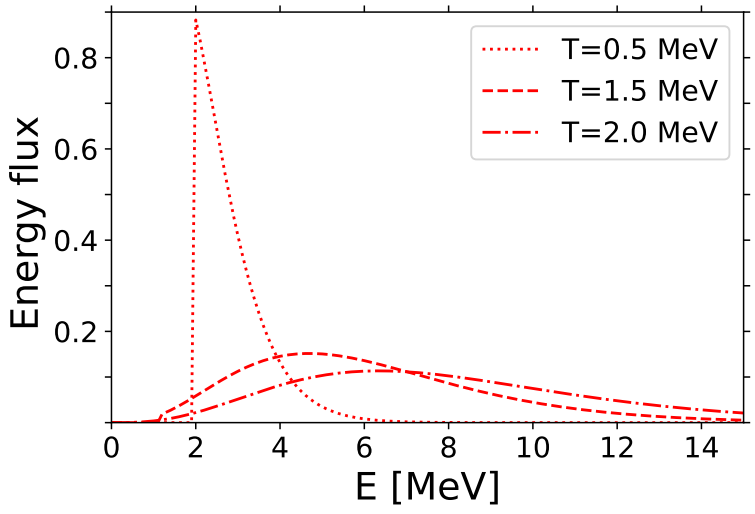

Fig. 6. Quasi-particle energy-flux (Eq. 18) as a function of the energy E. The vertical axis has been normalized by the total quasi-particle energy, and the flux is displayed for three different temperatures: $T = 0.5$ MeV (dotted line), $T = 1.5$ MeV (dashed line) and $T = 2$ MeV (dash-dotted line).

3.3. *Bosonic excitations of the neutrino plasma*

To explore the collective motion associated to pairs of neutrinos, one goes beyond the BCS approximation, by treating the terms H_{22} and H_{40+04} of Hamiltonian (8). The equations presented in Section 2.3 are then applied to the description of bosonic excitations in the neutrinosphere. The TDA approach gives energies $\omega_{\{n\}}$ (or ω in the continuum limit) which are also functions of the temperature. The temperature dependence of ω is shown in Figure 7. It has been calculated by solving Eq. 25. For the sake of the present discussion we have neglected ground-state correlations and we have limited ourselves to the TDA instead of the RPA (see Eq. 34). As can be seen from Figure 7, there is a region for $T < T_c$ which shows a gap in the spectrum of ω. This feature is also exhibited by the TDA energy distribution of Figure 8, where there is a threshold at low energies for $T < T_c$. The shift of the spectrum to lower energies follows the behaviour of the gap with the temperature. Beyond the critical temperature T_c, the TDA spectrum is similar to that of massless bosons.

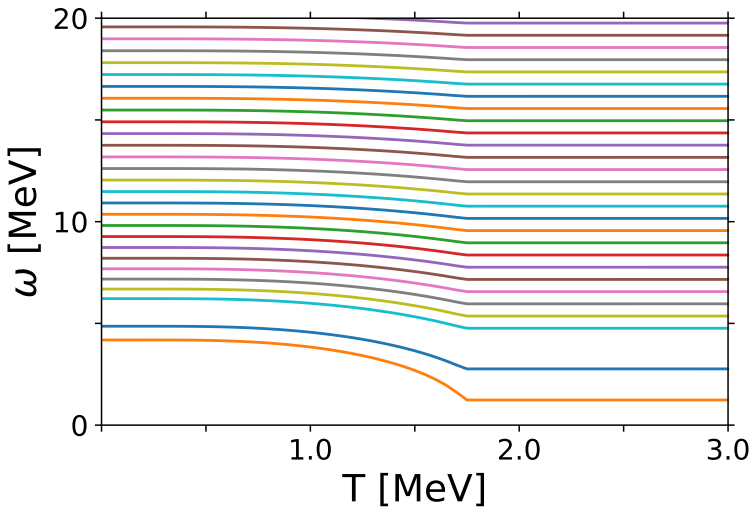

Fig. 7. Eigenvalues ω of the TDA equations (Eq. 21) as a function of the temperature.

Before ending this section we would like to make a comparison with the results reported by Birol et al. [18] in their paper. There, they have used the Richardson method to solve the pairing-interaction problem, a method which is suitable for the description of the short-range part of the pairing interaction. Here we have introduced a quasi-particle mean-field description consisting of the BCS method and the associated Bogoliubov transformations, followed by a TDA linearization of the long-range interactions among pairs of quasi-particles. In this respect, the combined procedure (BCS+TDA) allows a more complete description in both sides of the superfluid to normal regimes. This leads to a different behaviour of the exci-

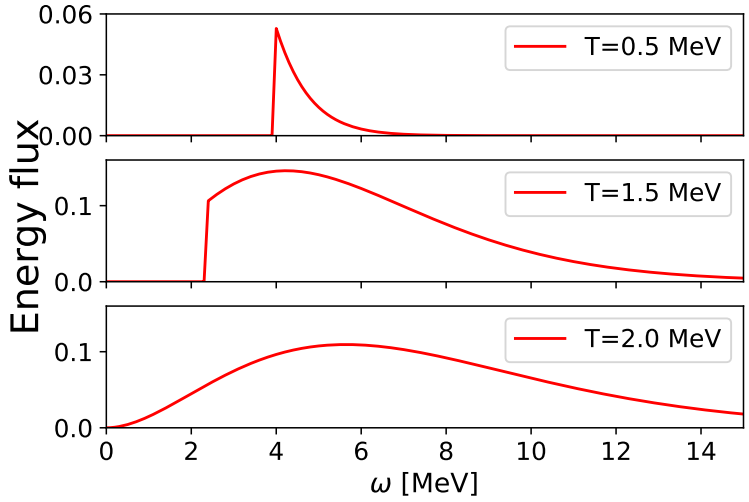

Fig. 8. Energy flux in the Tamm-Dancoff approximation (Eq. 38), as a function of the collective energies ω. The plot is shown for three different temperatures: $T = 0.5$ MeV (upper panel), $T = 1.5$ MeV (middle panel) and $T = 2$ MeV (lower panel).

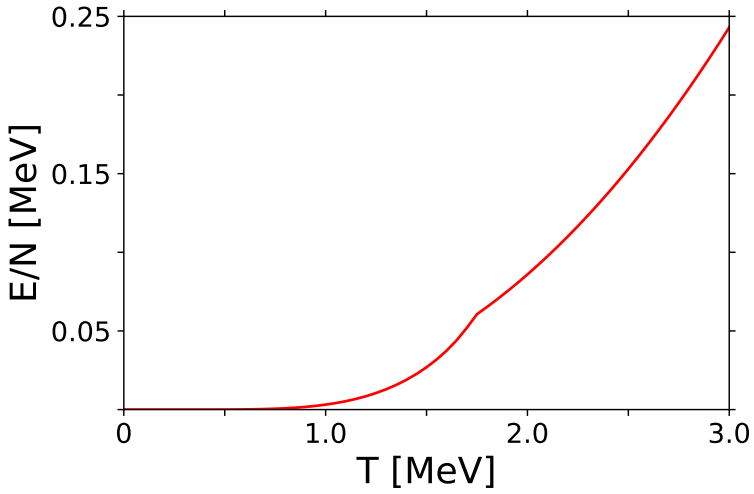

Fig. 9. Mean energy per particle in the Tamm-Dancoff approximation (Eq. 37)

tation energies with temperature and to the appearance of temperature-dependent low-energy thresholds for the emission of the neutrinos, in both the normal and superfluid phases.

4. Conclusions

In this work we have explored some consequences of the inclusion of pair-interactions among neutrinos within a SN environment, motivated by the ideas originally presented by S. Birol, Y. Pehlivan, A. Balantekin and T. Kajino [18]. Along the same lines, we have taken a separable pairing interaction but treated it in the BCS+TDA approximation. As a result of this approach, it is found that the spectral distribution of the emitted neutrinos shows the effect of the interactions both in the superfluid ($T < T_c$) and normal ($T > T_c$) phases. We think that this may be relevant for the analysis of the energy distribution of SN-neutrinos. From a physical point of view, the occurrence of neutrino-pair interactions would reflect upon the thermodynamic properties of the neutrinosphere, mostly affecting the heat transfer from the core to the external crust of the SN. It may also pave the way to the inclusion of more realistic interactions among neutrinos, particularly of the local type. Work is in progress concerning this aspect of the problem.

Acknowledgements

This work has been partially supported by the National Research Council of Argentina (CONICET) by the grant PIP 616, and by the Agencia Nacional de Promoción Científica y Tecnológica (ANPCYT) PICT 140492. M.P.C is a doctoral fellow of the CONICET. O.C. and A.V.P. are members of the Scientific Research career of the CONICET.

References

1. F. H. Shu and P. A. Hughes, *Nature* **357** (May 1992) 122.
2. H.-T. Janka, Neutrino Emission from Supernovae, in *Handbook of Supernovae*, eds. A. W. Alsabti and P. Murdin 2017, p. 1575.
3. G. G. Raffelt, Neutrino Masses in Astrophysics and Cosmology, in *Physics with Neutrinos*, ed. M. P. Locher (November 1996), p. 69.
4. A. V. Penacchioni and O. Civitarese, *ApJ Letters* **871** (February 2019) L30, arXiv:1904.07212 [astro-ph.HE].
5. W. Bednarek, High energy neutrinos from binary systems of two massive stars, International Cosmic Ray Conference (ICRC29) Vol. 5 (January 2005), p. 71.
6. E. Grohs, G. M. Fuller and M. Sen, *JCAP* **2020** (July 2020) 001, arXiv:2002.08557 [astro-ph.CO].
7. M. Bhatt, I. Sushch, M. Pohl, A. Fedynitch, S. Das, R. Brose, P. Plotko and D. M. A. Meyer, *Astroparticle Physics* **123** (December 2020) 102490, arXiv:2006.07018 [astro-ph.HE].
8. V. Brdar, M. Lindner, S. Vogl and X.-J. Xu, *Phys. Rev. D* **101** (June 2020) 115001, arXiv:2003.05339 [hep-ph].
9. Super-Kamiokande Collaboration, S. Fukuda, Y. Fukuda, T. Hayakawa and J. Kameda et al., *Nuclear Instruments and Methods in Physics Research A* **501** (April 2003) 418.

10. Y. Takeuchi and Super-Kamiokande Collaboration, *Nuclear Instruments and Methods in Physics Research A* **952** (February 2020) 161634.
11. Y. Kudenko, *arXiv e-prints* (May 2020) arXiv:2005.13641, arXiv:2005.13641 [physics.ins-det].
12. M. G. Aartsen, M. Ackermann, J. Adams, J. A. Aguilar, M. Ahlers, M. Ahrens, D. Altmann and et al., *Journal of Instrumentation* **12** (March 2017) P03012, arXiv:1612.05093 [astro-ph.IM].
13. A. Mirizzi, I. Tamborra, H. T. Janka, N. Saviano, K. Scholberg, R. Bollig, L. Hüdepohl and S. Chakraborty, *Nuovo Cimento Rivista Serie* **39** (February 2016) 1, arXiv:1508.00785 [astro-ph.HE].
14. H. Nagakura, *arXiv e-prints* (August 2020) arXiv:2008.10082, arXiv:2008.10082 [astro-ph.HE].
15. Y. George, Dense matter physics, in *Encyclopedia of Physical Science and Technology (Third Edition)*, ed. R. A. Meyers (Academic Press, New York, 2003) pp. 305 – 334.
16. G. G. Raffelt and A. Y. Smirnov, *Phys. Rev. D* **76** (October 2007) 081301, arXiv:0705.1830 [hep-ph].
17. G. G. Raffelt and A. Y. Smirnov, *Phys. Rev. D* **76** (December 2007) 125008, arXiv:0709.4641 [hep-ph].
18. S. Birol, Y. Pehlivan, A. B. Balantekin and T. Kajino, *Phys. Rev. D* **98** (October 2018) 083002, arXiv:1805.11767 [astro-ph.HE].
19. R. W. Richardson and N. Sherman, *Nuclear Physics* **52** (April 1964) 221.
20. Y. Pehlivan, A. B. Balantekin, T. Kajino and T. Yoshida, *Physical Review D* **84** (Sep 2011).
21. Y. Pehlivan, A. Subaşı, N. Ghazanfari, S. Birol and H. Yüksel, *Physical Review D* **95** (Mar 2017).
22. A. V. Patwardhan, M. J. Cervia and A. B. Balantekin, *Physical Review D* **99** (Jun 2019).
23. C. Volpe, *International Journal of Modern Physics E* **24** (Sep 2015) 1541009.
24. P. Ring and P. Schuck, *The Nuclear Many-Body Problem* (Springer, 2004).
25. J. Bardeen, L. N. Cooper and J. R. Schrieffer, *Physical Review* **108** (December 1957) 1175.
26. O. Civitarese, R. A. Broglia and C. H. Dasso, *Annals of Physics* **156** (August 1984) 142.
27. F. Alasia, O. Civitarese and M. Reboiro, *Phys. Rev. C* **35** (February 1987) 812.
28. O. Civitarese, R. J. Liotta and T. Vertse, *Phys. Rev. C* **64** (November 2001) 057305.